Hypoxia Drives Centrosome Amplification in Cancer Cells via HIF1α-Dependent Induction of Polo-Like Kinase 4

Karuna Mittal[1], Jaspreet Kaur[1], Shaligram Sharma[1], Nivya Sharma[1], Guanhao Wei[1], Ishita Choudhary[1], Precious Imhansi-Jacob[1], Nagini Maganti[1], Shrikant Pawar[1], Padmashree Rida[2], Michael S. Toss[3], Mohammed Aleskandarany[3], Emiel A. Janssen[4], Håvard Søiland[5], Meenakshi. V. Gupta[6], Michelle D. Reid[7], Emad A. Rakha[3], and Ritu Aneja[1]

ABSTRACT

Centrosome amplification (CA) has been implicated in the progression of various cancer types. Although studies have shown that overexpression of PLK4 promotes CA, the effect of tumor microenvironment on polo-like kinase 4 (PLK4) regulation is understudied. The aim of this study was to examine the role of hypoxia in promoting CA via PLK4. We found that hypoxia induced CA via hypoxia-inducible factor-1α (HIF1α). We quantified the prevalence of CA in tumor cell lines and tissue sections from breast cancer, pancreatic ductal adenocarcinoma (PDAC), colorectal cancer, and prostate cancer and found that CA was prevalent in cells with increased HIF1α levels under normoxic conditions. HIF1α levels were correlated with the extent of CA and PLK4 expression in clinical samples. We analyzed the correlation between *PLK4* and *HIF1A* mRNA levels in The Cancer Genome Atlas (TCGA) datasets to evaluate the role of PLK4 and HIF1α in breast cancer and PDAC prognosis. High *HIF1A* and *PLK4* levels in patients with breast cancer and PDAC were associated with poor overall survival. We confirmed PLK4 as a transcriptional target of HIF1α and demonstrated that in PLK4 knockdown cells, hypoxia-mimicking agents did not affect CA and expression of CA-associated proteins, underscoring the necessity of PLK4 in HIF1α-related CA. To further dissect the HIF1α-PLK4 interplay, we used HIF1α-deficient cells overexpressing PLK4 and showed a significant increase in CA compared with HIF1α-deficient cells harboring wild-type PLK4. These findings suggest that HIF1α induces CA by directly upregulating PLK4 and could help us risk-stratify patients and design new therapies for CA-rich cancers.

Implications: Hypoxia drives CA in cancer cells by regulating expression of PLK4, uncovering a novel HIF1α/PLK4 axis.

Introduction

Centrosomes are cellular organelles involved in microtubule organization, especially during cell division. Centrosome amplification (CA) refers to aberrations in the size, shape, number, or position of the centrosomes within cells (1). CA is a hallmark of various cancers and is often correlated with aberrant karyotypes, genomic instability, disease progression, and poor patient prognosis (2–5). Defects in centrosome duplication, elongation, or maturation are the primary causes of CA (6, 7). Consecutive rounds of centrosome reproduction or concurrent formation of multiple daughter centrioles around preexisting centrioles lead to aberrant centrosome duplication and the subsequent formation of supernumerary centrosomes (8, 9).

Polo-like kinase 4 (PLK4), a member of the polo family serine/threonine kinases, is required for centriole biogenesis via phosphorylation and interaction with centriolar proteins (10, 11). Although PLK4 is expressed at low levels under normal conditions, its increased expression has been reported in multiple malignancies (12–15). It is well established that PLK4 deregulation alters centriole duplication and causes aberrant numbers of centrosomes in cells resulting in genomic instability and, consequently, tumorigenesis (16). Various protein–protein interactions [such as interactions with nuclear factor-kappa B (17), MTK1 (18), KAT2A/2B (19), CAND1 (20)] dictate PLK4 levels, activity, and stability (21). Previous studies have demonstrated that deregulation of several oncogenes or tumor suppressor genes that regulate PLK4 expression, including *KLF14* and *TP53*, can cause the formation of supernumerary centrosomes (22). Ablation of KLF14, a transcription factor that normally represses PLK4 expression, results in PLK4 upregulation and CA induction (23). p53 also negatively regulates the expression of PLK4, and similar to KLF14 ablation, p53 loss results in elevated PLK4 expression and CA (24). Furthermore, human papillomavirus type 16 (HPV-16) E6 and E7 oncoproteins have been shown to disrupt host cell cycle checkpoints, including p53 and pRb; these checkpoints are important for oncogenic transformation. By doing so, E6 and E7 lead to increased *PLK4* mRNA levels, disrupt centriole duplication, and induce CA (25, 26).

Apart from the aforementioned cellular factors that affect centrosome function either directly or through master regulators in the cell, the hypoxic tumor microenvironment plays a key role in deregulating the expression of several centrosome-associated genes (27). We and others have previously shown that hypoxia upregulates CA-associated proteins, such as Aurora A and PLK4 (28, 29). Importantly, the Ward

[1]Department of Biology, Georgia State University, Atlanta, Georgia. [2]Novazoi Theranostics, Inc., Rancho Palos Verdes, California. [3]University of Nottingham and Nottingham University Hospitals, Nottingham, United Kingdom. [4]Stavanger University Hospital, Stavanger, Norway. [5]Department of Breast and Endocrine Surgery, Stavanger University Hospital, Stavanger, Norway. [6]Chestatee Pathology Associates, PC, Lawrenceville, Georgia. [7]Emory University School of Medicine, Atlanta, Georgia.

Note: Supplementary data for this article are available at Molecular Cancer Research Online (http://mcr.aacrjournals.org/).

K. Mittal and J. Kaur contributed equally to this article.

Corresponding Author: Ritu Aneja, Department of Biology, Georgia State University, 100 Piedmont Avenue, Atlanta, GA 30303. Phone: 404-413-5417; Fax: 404-413-5301; E-mail: raneja@gsu.edu

Mol Cancer Res 2022;20:596–606

doi: 10.1158/1541-7786.MCR-20-0798

This open access article is distributed under Creative Commons Attribution-NonCommercial-NoDerivatives License 4.0 International (CC BY-NC-ND).

©2021 The Authors; Published by the American Association for Cancer Research

& Hudson's study showed that in the presence of hypoxia and reactive oxygen species (ROS), both PLK1 and PLK4 were repressed in *TP53* wild-type (WT) cells. In contrast, in *TP53* null cells, PLK4 protein levels were elevated under the same conditions (30). Another study showed that hypoxia-regulated TrkAIII, an alternative TrkA splice variant, differentially phosphorylates several centrosome-associated components enhancing centrosome interaction with PLK4 while decreasing their interaction with separase, ultimately causing CA (31). However, the detailed molecular mechanisms undergirding the induction of CA remain poorly understood. While certain studies showed that the induction of CA was p53-dependent (32), others suggested a cancer type-specific effect of hypoxia on CA (33, 34). Taken together, the above studies suggest that CA is the result of a complex interplay between centrosome regulators like PLK4, hypoxia, and the status of key tumor suppressors such as p53 within cells. In this study, we evaluated the mechanisms underlying hypoxia-induced CA in cells from different tumor types and p53 mutation status. Our results suggest that hypoxia drives CA in cancer cells by regulating the expression of PLK4, uncovering a novel hypoxia-inducible factor-1α (HIF1α)/PLK4 axis that can be utilized for cancer diagnosis and treatment.

Materials and Methods

Immunofluorescence staining

Formalin-fixed, paraffin-embedded breast, colon, pancreatic, and prostate cancer tissue sections were deparaffinized, cleared in xylene (3X), and rehydrated in a series of decreasing ethanol concentrations. Antigen retrieval was performed in citrate buffer (pH 6) at 15 psi for 3 minutes. Tissues were incubated with 10% goat serum and then with γ-tubulin (1:1000 dilution) primary antibody for 1 hour. After washing with PBS, tissues were incubated with Alexa 555 anti-mouse secondary antibody (1:2000) for 1 hour. Washing with PBS was followed by counterstaining of nuclei with Hoechst. The coverslips were mounted using ProLong Gold AntiFade Reagent.

Microscopy and quantification of centrosome amplification

Fluorescent images of cells and tissue samples were captured using a Zeiss LSM700 confocal microscope. Images were processed using Zen software as described previously (4, 35–37). The number of γ-tubulin foci was used to measure CA as γ-tubulin is present in both the centrioles and pericentriolar matrix (PCM). CA was calculated as the percentage of cells with amplified centrosomes (presence of more than 2 centrosomes/cell) out of the total number of cells counted in 10 randomly selected fields (approximately 500 cells).

IHC, scoring, and weighted index for clinical specimens

Deparaffinization and antigen retrieval was carried out as described for immunofluorescence (IF) staining. Tissue sections were blocked with Ultravision Protein Block (Thermo Fisher Scientific) for 30 minutes, followed by Ultravision Hydrogen Peroxide Block (Thermo Fisher Scientific) for 10 minutes. Samples were incubated with primary antibodies against HIF1α (1:1000) or PLK4 (1:500) for 1 hour and then washed with Tris-buffered saline and Tween 20 (TBST). Samples were then incubated with an anti-rabbit horseradish peroxidase (HRP) secondary antibody (Biocare) for 1 hour. Signal detection was performed using the Universal DAB chromogen kit (Biocare). The staining intensity was scored as 0 (no signal), 1 (low signal), 2 (moderate signal), or 3 (high signal); the percentage of positive cells from ten randomly selected fields (approximately 500 cells) was determined. The product of the staining intensity and the percent of positive cells constituted the weighted index (WI).

Cell culture

Prostate cancer (PC-3 and DU145), pancreatic ductal adenocarcinoma (PDAC; CFPAC-1 and Capan-1), colorectal cancer (CRC; SW480 and HCT116), and breast cancer (MDA-MB-231 and MDA-MB-468) cells were purchased from ATCC. The cell lines were authenticated by DNA profiling. All the cell lines used were *Mycoplasma* negative detected by MycoSEQ *Mycoplasma* detection system (Thermo Fisher Scientific) which is a real-time PCR–based method. Additionally, all the cells used were in early passages, no passage longer than 10th passage was used. MDA-MB-231, Capan-1, CFPAC-1, and SW480 cells were maintained in DMEM medium; MDA-MB-468 in MEM; PC-3 and DU-145 cells in RPMI; HCT116 cells in McCoys 5A. Cell culture media were supplemented with 10% fetal bovine serum and 1% penicillin/streptomycin. All cell lines were maintained at 37°C in a humified 5% CO_2 atmosphere.

Mimicking hypoxic conditions and HIF1α overexpression

To induce hypoxia pharmacologically, we treated cells with 100 μmol/L of $CoCl_2$ for 24 hours. HIF1α was overexpressed by transfecting cells with a plasmid encoding GFP-tagged degradation-resistant HIF1α. The plasmid HA-HIF1α P402A/P564A-pcDNA3 was a generous gift from Dr. Willian Kaelin (Addgene plasmid #18955). Cells at approximately 70% confluency were transfected using Lipofectamine LTX according to the manufacturer's instructions.

Immunocytofluorescence staining

Cells grown on poly-L-lysine-coated cover glasses were fixed with ice-cold methanol for 10 minutes and blocked with 5% BSA 1XPBS/0.05% Triton X-100 and 10% goat serum for 30 minutes. Cells were incubated with primary antibodies against α-tubulin and γ-tubulin (1:1000 dilution) for 35 minutes. Subsequently, cells were washed with PBS and incubated with Alexa-555 and Alexa-488 conjugated antibodies (Invitrogen) at 37°C for 35 minutes. After staining with Hoechst 33342 (Invitrogen), cells were mounted onto glass slides with ProLong Gold Antifade Reagent.

Cell lysate preparation and immunoblotting

Western blot assay was performed as described previously (4, 36). Briefly, cells at 70% to 80% confluency were scraped with 1X RIPA cell lysis buffer [1 mmol/L β-glycerophosphate, 20 mmol/L Tris-HCl (pH 7.5), 1 mmol/L Na_2EDTA, 1 mmol/L Na_3VO_4, 150 mmol/L NaCl, 1 mmol/L EGTA, 2.5 mmol/L $Na_4P_2O_7$, 1 μg/mL leupeptin, 1% Triton, 10% protease inhibitor]. Proteins were separated by 10% SDS-PAGE and then transferred onto polyvinylidene fluoride membranes (Millipore). Immune-reactive bands were visualized using a Pierce enhanced chemiluminescence (ECL) detection kit (Thermo Fisher Scientific); β-actin was used as a loading control. Information pertaining to antibodies used is detailed in Supplementary Table S1.

qRT-PCR

Total RNA was extracted using TRIzol (Takara Bio, Inc.). Two micrograms of RNA and oligo-dT primers were used for cDNA synthesis in a total reaction volume of 10 μL. qRT-PCR reactions were prepared using SYBR-Green PCR Master Mix (Thermo Fisher Scientific) and run on a StepOnePlus Real-Time PCR system (Applied Biosystems; Thermo Fisher Scientific) Relative mRNA levels were calculated using the 2-ΔΔCt method. Primers sequences are provided in Supplementary Table S2.

PLK4 siRNA transfection and generation of HIF-1α knockout cells

For PLK4 knockdown (KD), ON-TARGETplus human PLK4 siRNAs (Dharmacon) were transfected according to the manufacturer's protocol. Briefly, cells at approximately 70% confluency were transfected with 30 pmol PLK4 siRNA under hypoxic ($CoCl_2$) or normoxic conditions. HIF1α gene knockout (KO) was performed using KN2.0 non–homology-mediated CRISPR KO kit (KN402461, Origene) according to the manufacturer's protocol. The target sequence of the HIF1α guide RNA (gRNA) vector (KN402461G1) was TTCTTTACTTCGCCGAGATC. The linear donor DNA (KN402461D) contained a LoxP-EF1A-tGFP-P2A-Puro-LoxP sequence. This single vector containing Cas9 and single-guide RNA (sgRNA) sequences was cotransfected with linear DNA (donor DNA) as per the manufacturer's protocol. The Cas9-mediated genome cutting was repaired by the integration of predesigned linear donor DNA containing the selection (Puromycin) and a reporter gene (GFP) via nonhomologous end joining repair. Cells at approximately 70% confluency were transfected with 1 μg each of guide RNA and donor DNA diluted in 250 μL OPTI-MEM (Invitrogen) using Lipofectamine LTX. After 48 hours, cells were split (1:5) and grown for 3 days. Cells at passage five were treated with 0.5 to 1 μg/mL puromycin to select for the clones with stable integration of the donor cassette. HIF-1α KO in puromycin-resistant clones was confirmed by qRT-PCR.

In vitro invasion and migration assays

Invasion and migration assays were performed using 24-well transwell plates with or without matrigel (Corning). Breast cancer (MDA-MB-231), PDAC (CFPAC-1), prostate cancer (PC-3), and colorectal cancer (HCT116) cells were treated ($CoCl_2$ or $CoCl_2$+ PLK4 siRNA) for 48 hours. Similarly, HIF1α KO MDA-MB-231, CFPAC-1, PC-3, and HCT116 cells were collected 48 hours after transfection with PLK4 overexpression (OE) or PLK4 control plasmids. Cells (2×10^4/L for invasion and 3×10^4/mL for migration) were resuspended in serum-free cell culture medium and seeded onto the top chamber. Subsequently, 500 μL of the respective cell culture medium supplemented with 20% FBS was added to the bottom chamber as a chemoattractant. After 24 hours, the cells that invaded the matrigel or migrated to the bottom surface of the transwell membrane were fixed with 70% methanol, stained using 0.1% crystal violet, and counted in ten random fields using a 20X objective.

Chromatin immunoprecipitation assay

MDA-MB-231, CFPAC-1, PC-3, and HCT116 were seeded (2.5×10^6) and transfected with degradation-resistant HIF1α OE and control plasmids. After 48 hours, cells were harvested for chromatin immunoprecipitation (ChIP). Briefly, cells were cross-linked with 1% formaldehyde; cross-linking was stopped using 0.125 M glycine. Cells were lysed, and the nuclear fraction was sonicated to shear the cross-linked DNA into approximately 500 bp fragments. The sonicated lysates were precleared with salmon-sperm coated agarose beads at 4°C for 1 hour. Half of the lysates were immunoprecipitated using 5 μg of the HIF1α antibody while the remaining lysates were immunoprecipitated using control (IgG) antibody; 1% of the lysates served as input. Samples were isolated by Protein A/salmon sperm beads and washed in increasing salt concentration buffers (low salt, high salt, LiCl, and 1X TE buffers) followed by DNA elution and reversal of cross-links (overnight incubation with 5M NaCl at 65°C followed by proteinase K treatment at 45°C). Immunoprecipitated DNA was isolated using a phenol: chloroform: isopropanol mixture (Invitrogen). Following extraction, samples were analyzed by qPCR.

Dual-luciferase assay

The PLK4 promoter-luciferase reporter plasmid was created by GenScript (details in Supplementary Methods). Cells were cotransfected with 500 ng of PLK4 plasmid and 500 ng of pRL-TK plasmids. Cells were also cotransfected with VEGF reporter plasmids with the pRL-TK plasmid as controls. Subsequently, cells were transfected with a degradation-resistant HIF1α OE or control plasmid using Lipofectamine 2000 (Invitrogen). After 48 hours, cells were harvested, and firefly and Renilla luciferase activities were measured using a dual-luciferase reporter assay system (Promega) and a luminometer (Perkin Elmer Victor 3). Firefly luciferase activity was normalized to that of Renilla. Each sample was analyzed in quadruplicates, and each transfection was repeated three times.

Statistical analysis

Statistical analyses were performed using GraphPad Prism or R software package. Two-tailed *t* tests were used for comparisons between two groups, whereas one-way ANOVA and Tukey multiple comparison tests were used for comparisons among three or more groups. *P* values less than 0.05 were considered statistically significant.

Results

HIF1α expression shows a strong positive correlation with CA and PLK4 levels in clinical specimens

We have previously shown that hypoxia promoted CA in breast tumors contributing to poor outcomes (29). In this study, we evaluated the relationship between hypoxia and CA in multiple other solid cancers, including prostate, pancreatic, and colorectal cancer. To this end, we performed IHC staining in adjacent serial sections of breast cancer ($n = 24$), colorectal cancer ($n = 38$), prostate cancer ($n = 52$), and PDAC ($n = 34$) tissue samples to assess the expression of nuclear HIF1α and cytoplasmic PLK4, a CA-associated protein (**Fig. 1A** and **B**). Adjacent serial sections from the same tumors were also immunofluorescently labeled for γ-tubulin (**Fig. 1C**), and CA was calculated as described previously (35). Statistical analysis revealed a strong positive correlation between nuclear HIF1α and CA in all tumor samples (Spearman rho and *P* values are shown in **Fig. 1D**). We also found a strong positive correlation between nuclear HIF1α and PLK4 in all the tumor samples (**Fig. 1D**). Descriptive statistics of the patient and clinicopathologic characteristics are provided in Supplementary Table S3.

To strengthen our clinical findings, we analyzed publicly available gene expression data of breast cancer, PDAC, colorectal cancer, and prostate cancer. We evaluated the expression levels of eight CA-related and 27 hypoxia-associated genes in these patients (Supplementary Table S4). A cumulative score (CA8) was generated by adding the log-transformed values of the normalized gene expression of *CCND1*, *NEK2*, *PIN1*, *TUBG1*, *PLK1*, *BIRC5*, *PLK4*, *and AURKA*. The patients were stratified into high and low CA8 groups (threshold based on log-rank test). Next, we assessed the expression of 27 hypoxia-associated genes (ref. 38; *ALDOA, ANGPTL4, ANLN, BNC1, C20ORF20, CA9, CDKN3, COL456, DCBLD1, ENO1, FAM83B, FOSL1, GNAL1, HIG2, KCTD11, KR717, LDHA, MPRS17, P4HA1, PGAM1, PGK1, SDC1, SLC16A1, SLAC2A1, TPI1, VEGF*, and *HIF1A*) in the same datasets (TCGA) used for CA8 quantitation. Interestingly, we found a significantly higher expression of the 27 hypoxia-associated genes in the CA8-high groups of all tumor types ($P = 0.06$ in breast cancer, $P = 0.02$

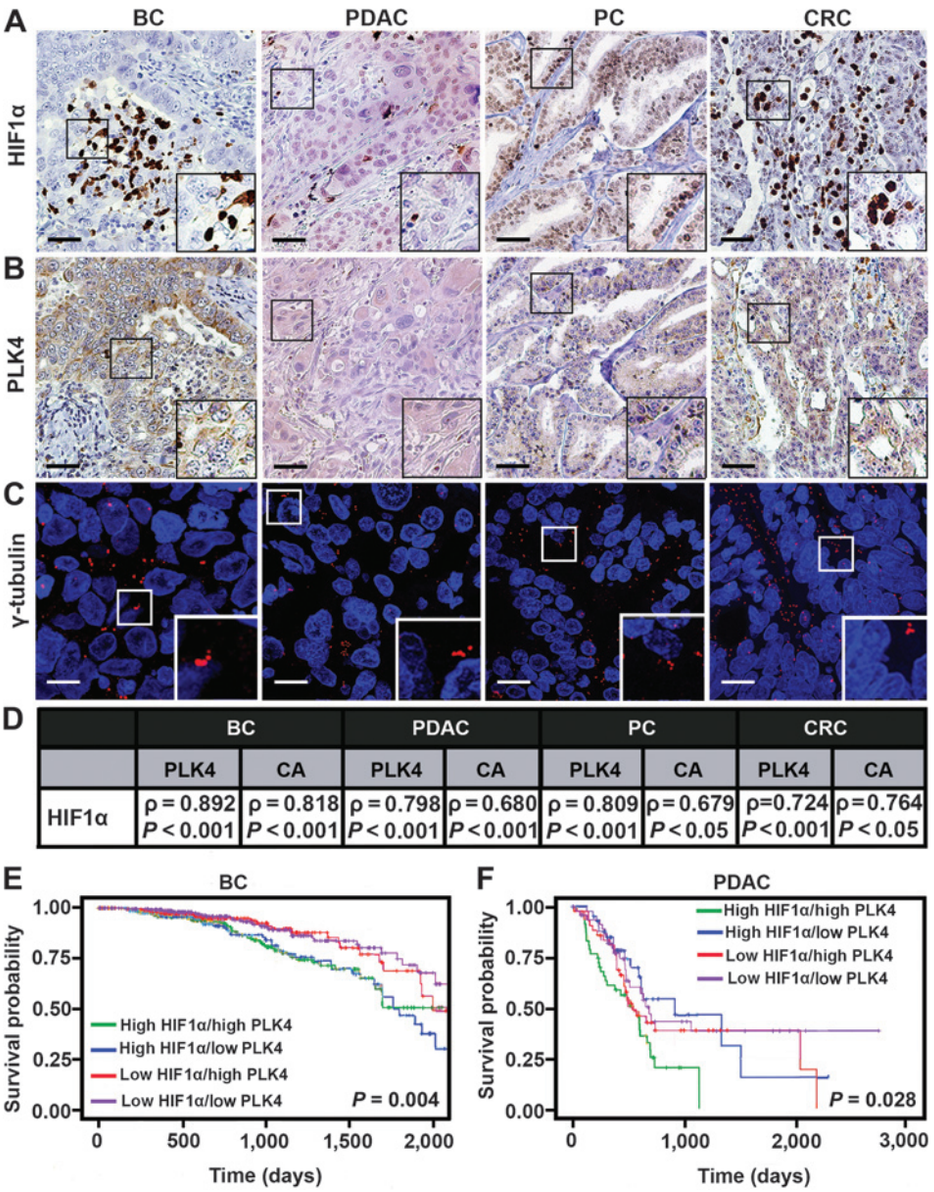

Figure 1.

High HIF1α expression is associated with high CA and PLK4 expression in clinical tumor samples. Representative IHC micrographs of breast cancer, PDAC, prostate cancer, and colorectal cancer tissue sections stained for HIF1α (**A**) and PLK4 (**B**). Scale bar (black), 50 μm. **C,** Confocal micrographs showing CA in breast cancer, PDAC, prostate cancer, and colorectal cancer tissue sections immunostained for centrosomes (γ-tubulin, red), and DNA was counterstained with Hoechst (blue). Scale bar (white), 20 μm. **D,** Table showing the Spearman rho and *P* values for CA, HIF1α, and PLK4 in breast cancer, PDAC, prostate cancer, and colorectal cancer tissue sections. Kaplan–Meier survival analysis showing OS in patients with breast cancer (**E**) and PDAC (**F**) stratified by *HIF1α* and *PLK4* expression levels (TCGA). BC, breast cancer; PC, prostate cancer; CRC, colorectal cancer.

in PDAC, $P < 0.001$ in patients with colorectal cancer, and prostate cancer; Supplementary Fig. S1A–S1D). In addition, after stratifying patients in *PLK4*-high and *PLK4*-low groups, we observed that *HIF1α* was expressed at higher levels in P*LK4*-high patients ($P < 0.05$ for all tumor types; Supplementary Fig. S1E–S1H).

Furthermore, we evaluated the relationship of *PLK4* and *HIF1A* levels (assessed by gene expression data) with overall survival (OS) in different tumor types. *HIF1A* and *PLK4* levels stratified patients with breast cancer and PDAC into high- and low-risk groups. Notably, the HIF1α-high/PLK4-high group had significantly poorer OS ($P = 0.04$) than HIF1α-high/PLK4-low, HIF1α-low/PLK4-high, and HIF1α-low/PLK4-low groups of patients with breast cancer (**Fig. 1F**). Similar trends were observed for PDAC. Patients with high HIF1α and PLK4 levels had significantly worse OS ($P = 0.028$) than HIF1α-high/PLK4-low (HR = 0.4701, $P = 0.0142$), HIF1α-low/PLK4-high (HR = 0.6497, $P = 0.1102$), and low-HIF1α/low-PLK4 (HR = 0.5005, $P = 0.0141$) groups of patients with PDAC (**Fig. 1E**). Collectively, these findings from our clinical specimens and TCGA analyses suggest that the hypoxic tumor microenvironment is accompanied by enhanced CA and increased PLK4 expression levels in different tumor types and contributes to poor OS.

Hypoxia-induced CA in solid cancers is mediated through HIF1α

Having established the strong correlation between HIF1α and CA in clinical specimens from different tumor types, we next examined the relationship between hypoxia and CA in cultured cells by mimicking hypoxic conditions using $CoCl_2$. To this end, we treated prostate cancer (PC-3 and DU145), PDAC (CFPAC-1 and Capan-1), colorectal cancer (SW480 and HCT116), and breast cancer (MDA-MB-231 and MDA-MB-468) cells with $CoCl_2$. $CoCl_2$-induced HIF1α stabilization led to a significant ($P < 0.05$) increase in the percentage of cells with numerical CA (approximately 1.6-fold in breast cancer, prostate

cancer, and colorectal cancer; approximately 1.8-fold in PDAC) compared with untreated cells (**Fig. 2A** and **B**; Supplementary Fig. S2A and S2B; Supplementary Table S7), as shown by confocal microscopy. Increased CA in $CoCl_2$-treated cells was further confirmed by the elevated levels of CA-associated proteins (pericentrin, PLK4, and Aurora A kinase; Supplementary Fig. S2D; Supplementary Table S5). Hypoxia was confirmed by HIF1α upregulation at the protein and mRNA levels (**Fig. 2C**; Supplementary Fig. S2C and S2D). qPCR and immunoblot (**Fig. 2C** and **D**; Supplementary Fig. S2C and S2D) also support our observation that PLK4 protein and mRNA levels increase with elevated levels of HIF1α upon treatment with $CoCl_2$ in MDA-MB 468, Capan-1, CFPAC-1, DU145, PC-3, and SW480 cells. A moderate change in the protein and mRNA levels of PLK4 was observed in MDA-MB-231 and HCT116 cells (**Fig. 2C** and **D**; Supplementary Fig. S2C and S2D).

To assess the involvement of HIF1α signaling in hypoxia-driven CA, we overexpressed GFP-tagged, degradation-resistant HIF1α in normoxic cultures. Cells transfected with HIF1α OE exhibited a higher frequency of CA (approximately 1.6 in breast cancer, prostate cancer, and colorectal cancer cells; approximately 1.8 in PDAC cells; Supplementary Fig. S3A and S3B), and elevated levels of CA-associated proteins (Supplementary Fig. S3C; Supplementary Table S5) than the ones transfected with vector controls under normoxic conditions. Mounting evidence suggests that *TP53* loss is associated with increased CA (2, 39, 40) and that p53 levels are associated with PLK4 expression (18, 41). Interestingly, we found that increased CA and CA-associated protein levels under hypoxic conditions (upregulation of HIF1α) in cancer cells were independent of *TP53* status, as indicated by the comparable increase (approximately 1.5-fold) in CA levels in *TP53* WT (HCT116), mutant (SW480), and null cells (HCT116 $TP53^{-/-}$) following $CoCl_2$ treatment/HIF1α OE (Supplementary Fig. S4). These data substantiate that the hypoxic tumor microenvironment enhances CA in cancer cells through HIF1α signaling.

Hypoxia-induced CA is dependent on HIF1α/PLK4 axis

To confirm the crucial role of PLK4 in driving CA under hypoxia, we assessed whether *PLK4* OE is sufficient to enhance CA. We depleted *HIF1A* using CRISPR/CAS9 and overexpressed *PLK4* in MDA-MB-231, CFPAC-1, PC-3, and HCT116 cells. CA induced 48 hours after PLK4 OE was confirmed by IF staining for γ-tubulin. PLK4 and HIF1α levels were evaluated by qRT-PCR (Supplementary Fig. S5). PLK4 OE resulted in significantly higher CA in the *HIF1A* KO cells (approximately 18%–29%) than in *HIF1A* KO/*PLK4* control vector (CV; approximately 7%–11%) or *HIF1A* WT (approximately 9%–18%) cells with endogenous *PLK4* expression (control) cultured under normoxic conditions (**Fig. 3A** and **B**). These findings suggest that *PLK4* OE is necessary and sufficient to enhance CA.

To further confirm that the increase in *PLK4* levels and CA in hypoxia is induced by HIF1α-mediated PLK4 upregulation, we transiently knocked down PLK4 using siRNA in MDA-MB-231, CFPAC-1, PC-3, and HCT116 cells and then treated these cells with $CoCl_2$. Treatment with $CoCl_2$ did not result in CA in *PLK4* KD cells, in

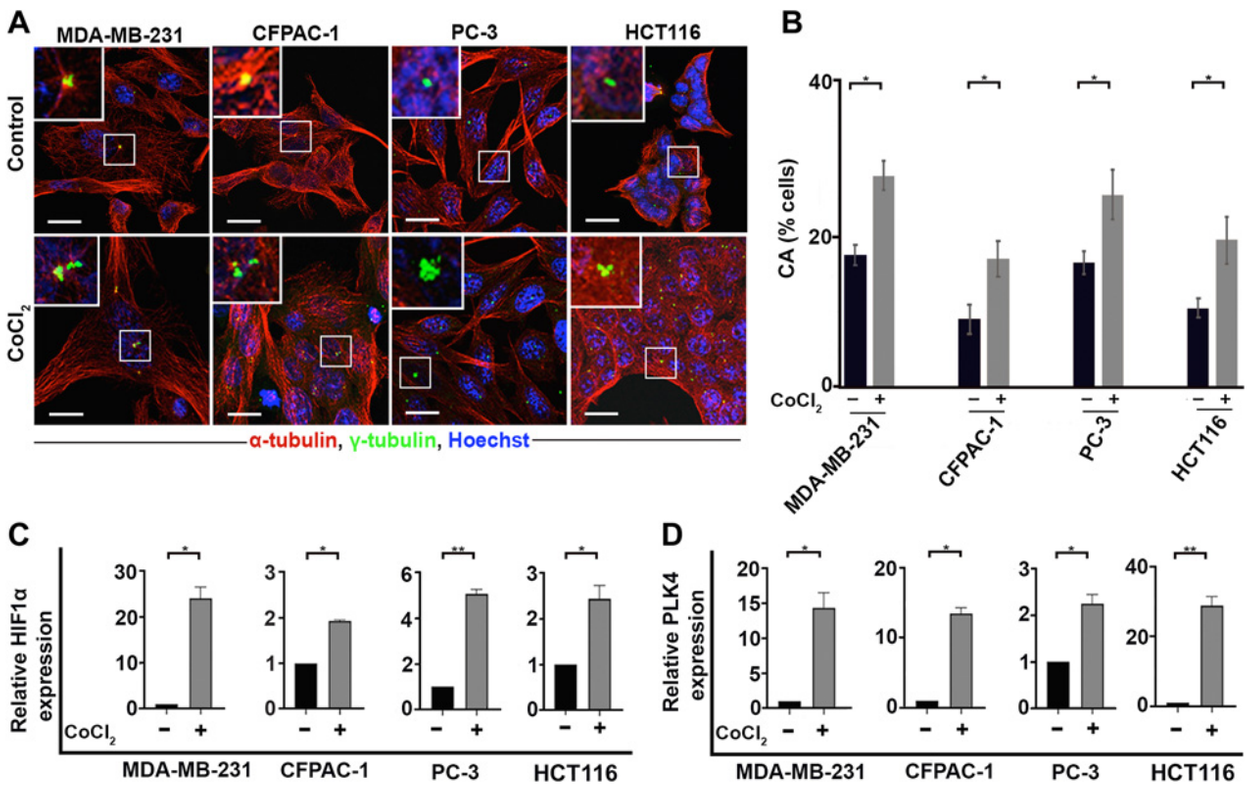

Figure 2.

Mimicking hypoxia using the HIF1α stabilizer $CoCl_2$ enhances CA. **A,** Confocal micrographs showing numerical CA. **B,** Bar-graph representing the quantitation of numerical CA. qRT-PCR analysis for *HIF1A* (**C**) and *PLK4* (**D**) mRNA levels in $CoCl_2$-treated (+) and control/untreated (−) MDA-MB-231, CFPAC-1, PC-3, and HCT116 cells. Data were normalized to *β-actin* mRNA levels. Centrosomes and microtubules were immunolabeled for γ-tubulin (green) and α-tubulin (red), respectively; DNA was counterstained with Hoechst (blue). Scale bar (white), 5 μmol/L. Error bars are means ± SD from triplicate data. Unpaired *t* test. $^*P < 0.05$.

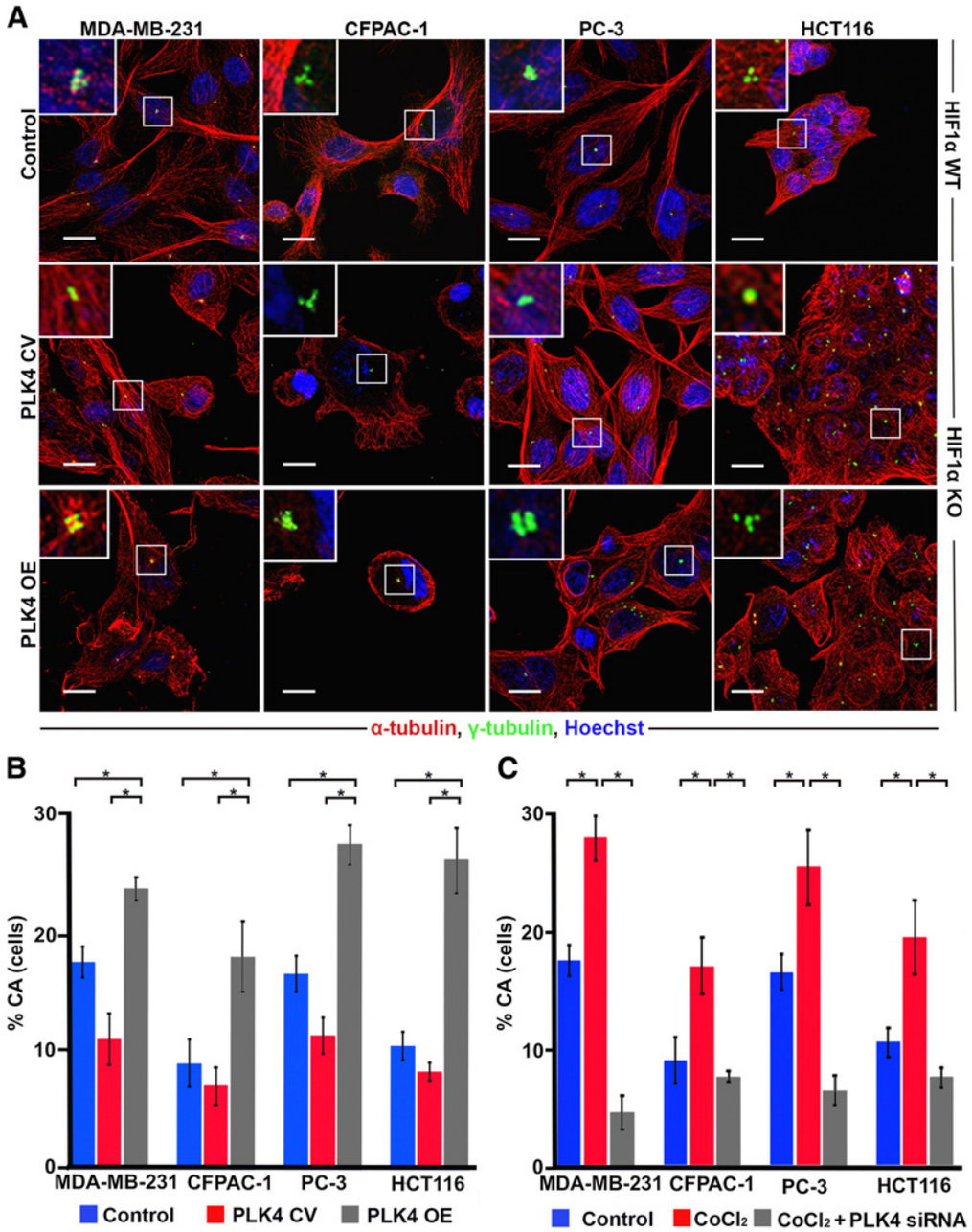

Figure 3.

A, Confocal micrographs showing numerical CA in control *(HIF1A* WT with endogenous PLK4 expression cultured in normoxic conditions) and *HIF1A* KO MDA-MB-231, CFPAC-1, PC-3, and HCT116 cells transfected with *PLK4* OE and control plasmids. Scale bar, 5 μmol/L. **B,** Bar-graphs representing the quantitation of numerical CA in control and *HIF1A* KO MDA-MB-231, CFPAC-1, PC-3, and HCT116 cells transfected with *PLK4* OE and control plasmids. Error bars are means ± SD from triplicate data. **C,** Bar-graphs representing the quantitation of numerical CA, in control, $CoCl_2$-treated, $CoCl_2$-treated/*PLK4* KD MDA-MB-231, CFPAC-1, PC-3, and HCT116 cells.

contrast to cells with WT *PLK4*, $CoCl_2$-treated (approximately 17%–28%) and control (approximately 9%–18%) cells (Supplementary Fig. S6A and **Fig. 3C**). The mRNA levels of *HIF1A* and *PLK4* under different conditions were evaluated by qRT-PCR (Supplementary Fig. S6B and S6C). The protein levels of PLK4 after PLK4 OE were evaluated by immunoblot assay (Supplementary Fig. S10; Supplementary Table S6). Collectively, these findings indicate that the increase in CA in hypoxia is mediated through the HIF1α/PLK4 axis.

Migration and invasion capacities of CA-rich hypoxic cancer cells are PLK4-dependent

Next, we examined the role of PLK4 in CA-mediated enhancement of the migratory and invasive capacity of hypoxic tumor cells. To this

end, we performed invasion and migration assays using *HIF1A* KO and WT MDA-MB-231, CFPAC-1, PC-3, and HCT116 cells. The overexpression of PLK4 in *HIF1A* KO cells significantly increased the number of cells that traversed the membrane (approximately 37%–56%) and matrigel (approximately 26%–43%) compared with *HIF1A* KO/*PLK4* CV (migration approximately 18%–24%, invasion approximately 10%–13%) or *HIF1A* WT/*PLK4* WT (migration approximately 19%–24%, invasion approximately 1%–11%) cells cultured under normoxic conditions (**Fig. 4A**–**H**). Migration and invasion capacities of control and *PLK4* OE or CV-transfected *HIF1A* KO MDA-MB-231, CFPAC-1, PC-3, and HCT116 cells were positively correlated with CA (**Fig. 4I**). Conversely, the number of cells that traversed the membrane and matrigel were significantly reduced (invasion approximately 5%–11%, migration approximately 16%–22%) by PLK4 KD in $CoCl_2$-treated cells when compared with $CoCl_2$-treated *PLK4* WT (invasion approximately 25%–41%, migration approximately 52%–65%) and control (invasion approximately 10%–21%, migration approximately 19%–32%) cells (Supplementary Fig. S7A–S7H). CA correlated positively with the migration and invasion capacities of control, *PLK4* OE or CV-transfected *HIF1A* KO (**Fig. 4I**), $CoCl_2$-treated *PLK4 WT*, and $CoCl_2$-treated *PLK4* KD, MDA-MB-231, CFPAC-1, PC-3, and HCT116 cells (Supplementary Fig. S7I). Together, these findings suggest that the enhanced migratory and invasive capabilities of tumor cells with supernumerary centrosomes under hypoxic conditions are PLK4-dependent.

HIF1α transcriptionally upregulates PLK4 to induce CA

Having demonstrated the correlation between PLK4 and HIF1α and the increase in CA in response to hypoxia in a HIF1α-dependent manner, we next assessed whether HIF1α is a direct regulator of *PLK4*. To determine this, we evaluated the potential transcriptional regulation of PLK4 by HIF1α. To assess the binding of HIF1α to the *PLK4* promoter, we used publicly available ChIP sequencing (ChIP-seq) data (42, 43, 44) from cancer cells cultured under hypoxic conditions. We found significant occurrence of three putative HIF1α binding sites (45) at the gene-proximal promoter site, according to TRANSFAC analysis (Supplementary Materials and Methods; **Fig. 5A**; ref. 46). These data support our hypothesis

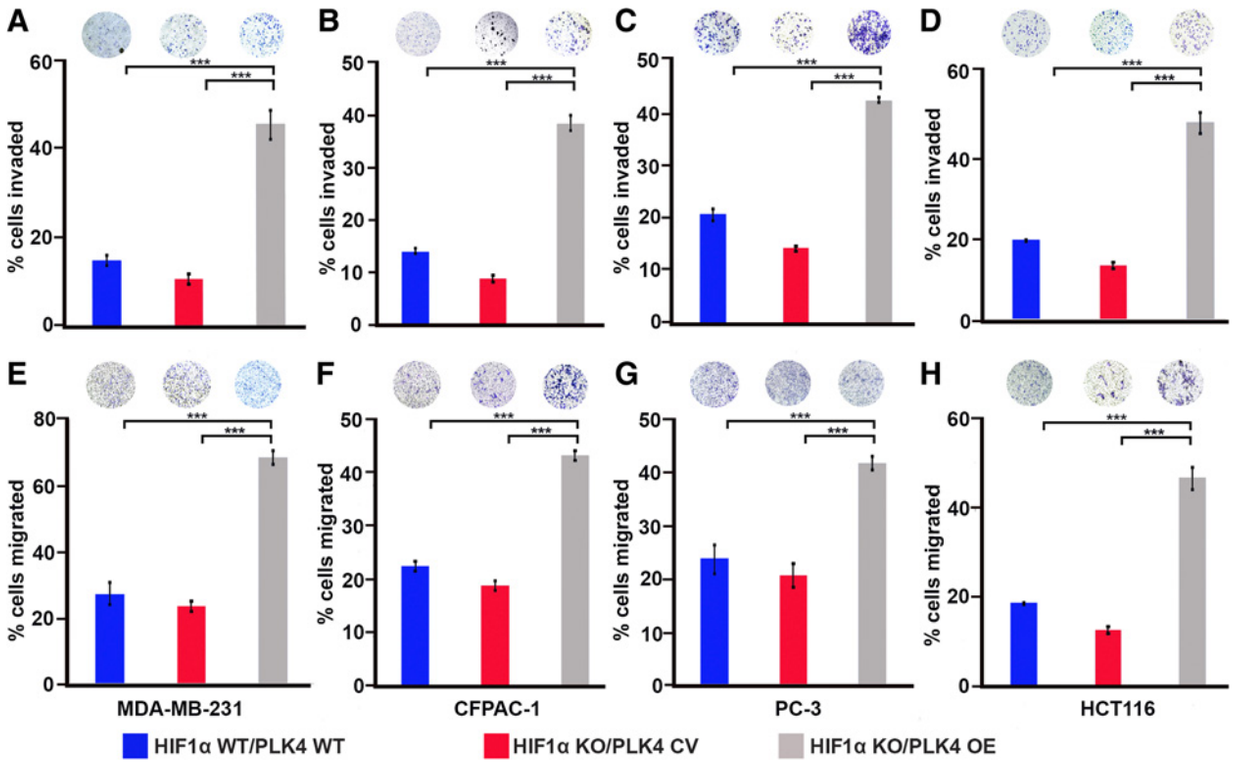

I

	Correlation between % CA and % cells invaded				Correlation between % CA and % cells migrated			
	MDA-MB-231	CFPAC-1	PC-3	HCT116	MDA-MB-231	CFPAC-1	PC-3	HCT116
Control	0.82 (<0.05)	0.98 (<0.001)	0.82 (<0.05)	0.93 (<0.05)	0.98 (<0.001)	0.82 (<0.05)	0.89 (<0.05)	0.81 (<0.05)
PLK4 CV	0.93 (0.012)	0.99 (0.01)	0.93 (<0.001)	0.88 (<0.001)	0.99 (<0.05)	0.99 (0.01)	0.97 (<0.05)	0.99 (<0.05)
PLK4 OE	0.91 (<0.001)	0.99 (<0.05)	0.88 (<0.05)	0.93 (0.01)	0.97 (<0.05)	0.95 (0.01)	0.99 (<0.05)	0.89 (<0.001)

Figure 4.
Hypoxia-induced CA increases cancer cell invasion and migration in a HIF1α/PLK4-dependent manner. Representative brightfield microscopic images and bar-graphs showing the invasion capacity (**A–D**) and migration capacity (**E–H**) of control, *PLK4* OE, and *PLK4* CV *HIF1A* KO MDA-MB-231 (**A** and **E**), CFPAC-1 (**B** and **F**), PC-3 (**C** and **G**), and HCT116 (**D** and **H**) cells. Data shown is means ± SD ($n = 3$), $^{*}P \le 0.05$, $^{**}P \le 0.01$, and $^{***}P \le 0.001$. **I,** Table showing the correlation between the percentage of cells with amplified centrosomes and percentage of cells invaded or migrated to the lower chamber under different experimental conditions.

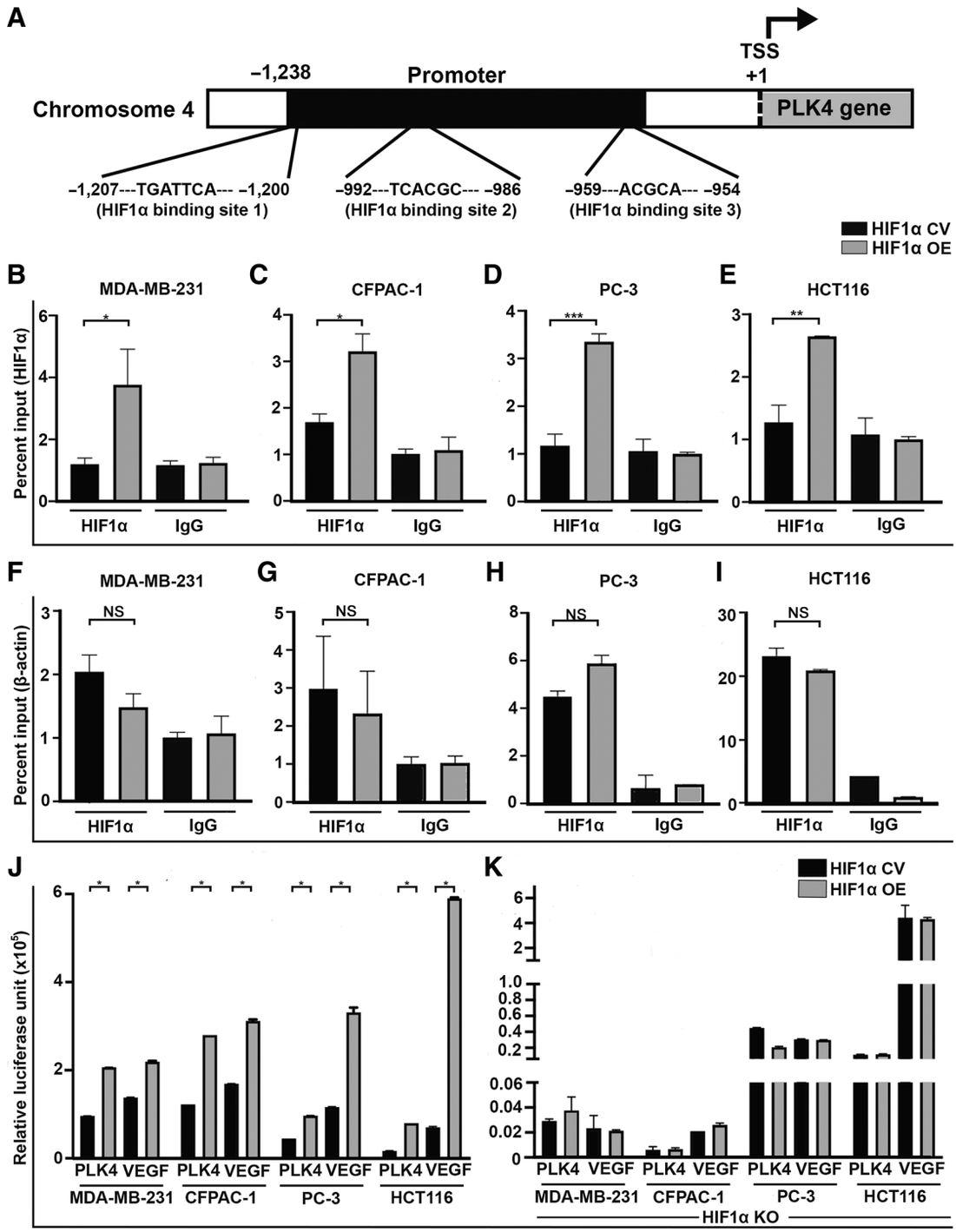

Figure 5.

HIF1α transcriptionally regulates the expression of *PLK4*. **A,** HIF1α binding sites in the *PLK4* promoter. **B,** Bar-graphs representing HIF1α binding on the *PLK4* promoter (**B–E**) and *β-actin* promoter (**F–I**) in MDA-MB-231 (**B** and **F**), CFPAC-1 (**C** and **G**), PC-3 (**D** and **H**), and HCT116 (**E** and **I**) cells transfected with control or degradation-resistant HIF1α-encoding plasmids. Bar-graph representing the relative luciferase activity from *PLK4* and *VEGF* promoter constructs in MDA-MB-231, CFPAC-1, PC-3, and HCT116 cells (**J**), as well as in *HIF1A* KO MDA-MB-231, CFPAC-1, PC-3, and HCT116 cells (**K**) transfected with control or GFP-tagged degradation-resistant HIF1α-encoding plasmids. Error bars are means ± SD from triplicate data. Unpaired *t* test. $^{*}P \leq 0.05$, $^{**}P \leq 0.01$. NS, not significant.

that HIF1α binds to the *PLK4* promoter in cancer cells under hypoxic conditions.

We performed ChIP to validate these *in silico* findings and confirmed HIF1α binding to the predicted binding sites in the promoter region of *PLK4* genes in breast cancer, PDAC, prostate cancer, and colorectal cancer cells. We found that HIF1α binding within the hypoxia response element (HRE) motifs was significantly higher in genomic DNA from MDA-MB-231, CFPAC-1, PC-3, HCT116 (**Fig. 5B–E**), and MDA-MB-468 (Supplementary Fig. S9) cells transfected with degradation-resistant HIF1α than in cells transfected with control vectors ($P < 0.05$). However, we did not find any significant differences in β-actin binding within HRE motifs from cells transfected with degradation-resistant HIF1α or in cells transfected with control vectors (**Fig. 5F–I**). We found that in presence of $CoCl_2$ also, HIF1α binding within the HRE motifs was significantly higher in genomic DNA from MDA-MB-231 and MDA-MB-468 (Supplementary Fig. S8).

Next, we performed a dual-luciferase reporter assay to confirm that HIF1α binding to the PLK4 promoter modulates PLK4 transactivation. Our results revealed significantly higher (approximately 3-fold) relative luciferase activity in HIF1α OE cells compared with CV cells for both *PLK4* and *VEGF* (positive control) reporters (**Fig. 5J**; $P < 0.05$). These data suggest that HIF1α transcriptionally upregulates *PLK4*. We further confirmed HIF1α-mediated upregulation of *PLK4* by selectively ablating *HIF1A* using CRISPR/CAS9 and exposing *HIF1A* KO cells to hypoxia or transfecting them with a degradation-resistant HIF1α-encoding plasmid. We found no significant difference in the relative luciferase activity for *PLK4* and *VEGF* promoter constructs in HIF1α OE or CV cells (**Fig. 5K**). Together, these results indicate that HIF1α binds to cis-HREs within the *PLK4* promoter and activates its expression.

Discussion

CA has been documented as a feature of human cancers and a valuable prognostic factor in various cancer types (2, 4, 5, 35). Although a few studies have focused on the targetable features of CA, including centrosome-dependent invasion, centrosome clustering, and centrosome inactivation, none of the molecules have made their way into clinical trials (47). The major bottleneck in the therapeutic utility of CA is the lack of understanding of the factors that induce CA in cancer cells.

Hypoxia, a major component of the tumor microenvironment, has recently emerged as a key factor in inducing CA. Tumor hypoxia is an essential regulator for the expression of genes involved in cell cycle regulation and tumorigenesis. Notably, the transcription factor HIF1α is a critical regulatory factor for over 100 genes. Among these genes, *VEGF*, *PGI*, *c-MET*, *CXCR4*, *CDC2*, *RB1*, *PAI-1*, *Aurora A/STK15*, *miRNA-210*, and *miRNA-34a* play a pivotal role in tumorigenesis, metastasis, and CA (35, 48). We have previously shown that increased hypoxia is associated with enhanced CA in breast cancer (29) and HPV-negative head and neck cancer cells (35), consistent with a previous study showing increased CA in endothelial cells exposed to hypoxia (32). Our present results show through a combination of *in vivo*, biochemical, and molecular experimental analyses that the extent of CA in human prostate cancer, PDAC, and colorectal cancer samples is associated with HIF1α and PLK4 expression levels. These findings were further corroborated by our *in silico* analyses showing that the high expression of CA-related genes was positively correlated with high hypoxia scores. The latter is supported by a recent study showing that the CA20 (49) is associated with hypoxia in cancer. Concordant with our previous work on hypoxia and CA (5, 29), we observed that high hypoxia and high CA were associated with poor OS in patients with breast cancer and PDAC. It is noteworthy that high HIF1α/high PLK4 subgroups had worse OS ($P < 0.05$) than the HIF1α-low/PLK4-high patients with breast cancer and PDAC. This finding suggests that high *HIF1A* levels were crucial in driving poor prognosis regardless of PLK4 status. Moreover, within the HIF1α-high group, PLK4 levels could further stratify patients with breast cancer and PDAC into high- and low-risk groups, raising the possibility that a combination of HIF1α and PLK4 inhibitors may work for this subgroup. This finding also spotlights the previously unrecognized role of the HIF1α/PLK4 axis in dictating poor prognosis.

Further, we confirmed that the extent of CA increased when breast cancer, prostate cancer, PDAC, and colorectal cancer cells were cultured in hypoxia-mimicking conditions. In accordance with our previous findings in breast cancer (29), the increase in CA was accompanied by elevated levels of CA-associated proteins, including Aurora A, PLK4, and pericentrin. However, there are conflicting reports regarding the role of hypoxia in the regulation of the expression of CA-associated proteins. A study in liver cancer cells showed that hypoxia and HIF1α upregulated the expression of the CA-associated gene *STK15 (*28), while another study in breast cancer showed that hypoxia promoted Aurora A downregulation (34). Hence, the role of hypoxia and HIF1α in the expression of CA-associated proteins may be tumor type-specific or may vary depending on the presence of different mutations. Moreover, multiple studies showed that loss of *TP53* was associated with increased CA and that p53 levels were negatively correlated with the levels of CA-associated proteins (2, 30). In this study, we demonstrated that hypoxia-induced CA in tumor cells through HIF1α-mediated PLK4 upregulation regardless of the p53 status and tumor type. We showed that *HIF1A* KO/*PLK4* OE cells exhibited significantly higher CA than *HIF1A* KO/*PLK4* CV or *HIF1A* KO cells cultured under normoxic conditions. In addition, $CoCl_2$-treated *PLK4* KD cells showed lower CA than *PLK4* WT, untreated cells, or $CoCl_2$-treated cells. These findings substantiate that the increase in CA under hypoxic conditions is mediated through the HIF1α/PLK4 axis. These findings have been confirmed in nine cell lines from four different tumor types in this study, providing a segue for studies utilizing patient-derived *in vitro* cancer models (e.g., organoids), which can effectively recapitulate the 3D architecture and intricate features of tumors and the tumor microenvironment.

Numerous studies have demonstrated that hypoxia is associated with an increased capacity for metastasis. We and others have shown that CA and increased PLK4 expression offer cytoskeletal advantages to the cells, resulting in increased directional migration and invasion. Although it is possible that hypoxia may promote metastasis by directly regulating genes involved in epithelial to mesenchymal transition, our results support the notion that hypoxia induces cancer cell migration and invasion via the HIF1α/PLK4 axis. Furthermore, our results show that the changes in migration and invasion capacities are positively correlated with the extent of CA in tumor cells under different culture conditions. Thus, we can infer that CA-induced cancer cell migration and invasion during hypoxic conditions are PLK4-dependent. Based on these lines of evidence, the notion that hypoxia-induced CA is responsible for driving the evolution of more aggressive phenotypes is plausible. Moreover, our finding that tumor cells are reliant on the HIF1α/PLK4 axis for migration provides possible mechanistic cues into why HIF1α/PLK4-high tumors are associated with poor OS. Altogether, our findings that PLK4 overexpression is HIF1α-dependent in hypoxic cancer cells may be useful in patient stratification and clinical decision-making.

Our study has uncovered a previously unrecognized link between HIF1α and PLK4 in the context of CA. Although previous studies have shown an indirect link between HIF1α and PLK4, the direct regulation of PLK4 by HIF1α has remained *hitherto* unknown. Our study has shown that HIF1α directly upregulates PLK4 under hypoxic conditions. Expression of degradation-resistant HIF1α in normoxic cancer cells was sufficient to upregulate PLK4. Conversely, *HIF1A* depletion profoundly reduced the mRNA levels of *PLK4*. Furthermore, our reporter assays confirmed *PLK4* promoter activity in cells expressing degradation-resistant HIF1α, which was abolished upon HIF1α depletion. These findings affirm through multiple experimental methodologies that HIF1α transcriptionally regulates PLK4. Our data do not preclude the "intersection" of the HIF1α/PLK4 axis with the known PLK4 regulatory mechanisms [DREAM–CDE/CHR pathway (50), nuclear factor-kappa B (17), E2F activators (51), KLF14 (24), and E6/E7 oncoproteins (9, 25)] under hypoxic conditions. Further studies are warranted to establish the crosstalk between HIF1α and PLK4.

While these findings position HIF1α and PLK4 as potential prognostic biomarkers in multiple cancers, they also highlight the possibility of their use as a viable combination as therapeutic targets. This lends support to the potential clinical value of HIF1α and PLK4 inhibitors to selectively target cancer cells exhibiting high levels of hypoxia and CA. A recent study showed that the PLK4 inhibitor CFI-400945 I (currently in phase I clinical trials; NCT01954316) inhibited tumor progression in pancreatic cancer patient-derived xenografts that exhibited high levels of hypoxia (52). Centrinone and Centrinone B are selective and reversible small-molecule inhibitors of PLK4, and they can deplete centrosomes in cell lines harboring varying levels of CA. The centrosome loss and the subsequent mitotic defects in cancer cells inhibited proliferation and promoted cell death, highlighting the potential use of PLK4 inhibitors as anticancer agents that reverse CA (53, 54). HIF inhibitors have been tested as single agents or in combination with other drugs, primarily for the treatment of advanced or refractory cancer. HIF inhibitors have shown promising results in the inhibition of tumor progression and cancer cell invasion (55). A recent study showed that PLK4 inhibition improved the antitumor effect of bortezomib (PS-341), a proteasome inhibitor that inhibits glioblastoma cell adaptation to hypoxia by targeting HIF1α (56). Taking into consideration these findings, we speculate that HIF1α and PLK4 inhibitors may selectively target cancer cells exhibiting CA and could suppress CA-induced chromosomal instability and metastasis.

This is the first report to substantiate the previously unrecognized role of hypoxia in inducing CA via HIF1α-mediated PLK4 upregulation. Given the recent progress in the development of HIF1α and PLK4 inhibitors, it is important to identify the patient population that could most benefit from HIF1α and PLK4 targeted therapies. Our findings also offer a novel parameter for the risk-stratification of patients and clinical decision-making while also furthering the design of novel therapy to target cancers with centrosomal aberrations.

Authors' Disclosures

P. Rida is the CEO of Novazoi Theranostics, Inc. but in the 36 months prior to publication, has not received any financial/nonfinancial support from Novazoi Theranostics, Inc. The patents held by Novazoi Theranostics, Inc. are not directly related to the subject matter of this publication. No disclosures were reported by the other authors.

Authors' Contributions

K. Mittal: Conceptualization, formal analysis, investigation, methodology, writing–original draft, writing–review and editing. **J. Kaur:** Investigation, methodology, writing–review and editing. **S. Sharma:** Formal analysis, methodology. **N. Sharma:** Methodology. **G. Wei:** Formal analysis. **I. Choudhary:** Formal analysis, methodology. **P. Imhansi-Jacob:** Methodology. **N. Maganti:** Methodology. **S. Pawar:** Methodology. **P. Rida:** Conceptualization. **M.S. Toss:** Resources. **M. Aleskandarany:** Resources. **E.A. Janssen:** Resources. **H. Søiland:** Resources. **M.V. Gupta:** Resources. **M.D. Reid:** Resources. **E.A. Rakha:** Resources. **R. Aneja:** Conceptualization, resources, supervision, writing–original draft, writing–review and editing.

Acknowledgments

This study was supported by grants to Ritu Aneja from the NCI of NIH (grant no. UO1 CA179671).

The costs of publication of this article were defrayed in part by the payment of page charges. This article must therefore be hereby marked *advertisement* in accordance with 18 U.S.C. Section 1734 solely to indicate this fact.

Received September 10, 2020; revised October 20, 2021; accepted December 14, 2021; published first December 21, 2021.

References

1. Nigg EA. Origins and consequences of centrosome aberrations in human cancers. Int J Cancer 2006;119:2717–23.
2. Chan JY. A clinical overview of centrosome amplification in human cancers. Int J Biol Sci 2011;7:1122–44.
3. Lingle WL, Barrett SL, Negron VC, D'Assoro AB, Boeneman K, Liu W, et al. Centrosome amplification drives chromosomal instability in breast tumor development. Proc Natl Acad Sci U S A 2002;99:1978–83.
4. Mittal K, Ogden A, Reid MD, Rida PC, Varambally S, Aneja R. Amplified centrosomes may underlie aggressive disease course in pancreatic ductal adenocarcinoma. Cell Cycle 2015;14:2798–809.
5. Pannu V, Mittal K, Cantuaria G, Reid MD, Li X, Donthamsetty S, et al. Rampant centrosome amplification underlies more aggressive disease course of triple negative breast cancers. Oncotarget 2015;6:10487–97.
6. D'Assoro AB, Lingle WL, Salisbury JL. Centrosome amplification and the development of cancer. Oncogene 2002;21:6146–53.
7. Marteil G, Guerrero A, Vieira AF, de Almeida BP, Machado P, Mendonça S, et al. Over-elongation of centrioles in cancer promotes centriole amplification and chromosome missegregation. Nat Commun 2018;9:1258.
8. Duensing A, Liu Y, Perdreau SA, Kleylein-Sohn J, Nigg EA, Duensing S. Centriole overduplication through the concurrent formation of multiple daughter centrioles at single maternal templates. Oncogene 2007;26:6280–8.
9. Duensing S, Lee LY, Duensing A, Basile J, Piboonniyom S-O, Gonzalez S, et al. The human papillomavirus type 16 E6 and E7 oncoproteins cooperate to induce mitotic defects and genomic instability by uncoupling centrosome duplication from the cell division cycle. Proc Natl Acad Sci U S A 2000;97:10002–7.
10. Sillibourne JE, Bornens M. Polo-like kinase 4: the odd one out of the family. Cell Div 2010;5:25.
11. Habedanck R, Stierhof YD, Wilkinson CJ, Nigg EA. The polo kinase Plk4 functions in centriole duplication. Nat Cell Biol 2005;7:1140–6.
12. Liao Z, Zhang H, Fan P, Huang Q, Dong K, Qi Y, et al. High PLK4 expression promotes tumor progression and induces epithelialmesenchymal transition by regulating the Wnt/betacatenin signaling pathway in colorectal cancer. Int J Oncol 2019;54:479–90.
13. Hu Z, Fan C, Oh DS, Marron J, He X, Qaqish BF, et al. The molecular portraits of breast tumors are conserved across microarray platforms. BMC Genomics 2006;7:96.
14. Li Z, Dai K, Wang C, Song Y, Gu F, Liu F, et al. Expression of polo-like kinase 4 (PLK4) in breast cancer and its response to taxane-based neoadjuvant chemotherapy. J Cancer 2016;7:1125–32.
15. Kawakami M, Mustachio LM, Zheng L, Chen Y, Rodriguez-Canales J, Mino B, et al. Polo-like kinase 4 inhibition produces polyploidy and apoptotic death of lung cancers. Proc Natl Acad Sci U S A 2018;115:1913–8.

16. Zhao Y, Wang X. PLK4: a promising target for cancer therapy. J Cancer Res Clin Oncol 2019;145:2413–22.
17. Ledoux A, Sellier H, Gillies K, Iannetti A, James J, Perkins N. NFkappaB regulates expression of polo-like kinase 4. Cell Cycle 2013;12:3052–62.
18. Nakamura T, Saito H, Takekawa M. SAPK pathways and p53 cooperatively regulate PLK4 activity and centrosome integrity under stress. Nat Commun 2013;4:1775.
19. Fournier M, Tora L. KAT2-mediated PLK4 acetylation contributes to genomic stability by preserving centrosome number. Mol Cell Oncol 2017;4:e1270391.
20. Korzeniewski N, Hohenfellner M, Duensing S. CAND1 promotes PLK4-mediated centriole overduplication and is frequently disrupted in prostate cancer. Neoplasia 2012;14:799–806.
21. Barr FA, Sillje HH, Nigg EA. Polo-like kinases and the orchestration of cell division. Nat Rev Mol Cell Biol 2004;5:429–40.
22. Nigg EA, Holland AJ. Once and only once: mechanisms of centriole duplication and their deregulation in disease. Nat Rev Mol Cell Biol 2018;19:297–312.
23. Fan G, Sun L, Shan P, Zhang X, Huan J, Zhang X, et al. Loss of KLF14 triggers centrosome amplification and tumorigenesis. Nat Commun 2015;6:8450.
24. Li J, Tan M, Li L, Pamarthy D, Lawrence TS, Sun Y. SAK, a new polo-like kinase, is transcriptionally repressed by p53 and induces apoptosis upon RNAi silencing. Neoplasia 2005;7:312–23.
25. Duensing S, Münger K. Human papillomaviruses and centrosome duplication errors: modeling the origins of genomic instability. Oncogene 2002;21:6241.
26. Korzeniewski N, Treat B, Duensing S. The HPV-16 E7 oncoprotein induces centriole multiplication through deregulation of polo-like kinase 4 expression. Mol Cancer 2011;10:61.
27. Mittal K, Aneja R. Spotlighting the hypoxia-centrosome amplification axis. Med Res Rev 2020;40:1508–13.
28. Klein A, Flugel D, Kietzmann T. Transcriptional regulation of serine/threonine kinase-15 (STK15) expression by hypoxia and HIF-1. Mol Biol Cell 2008;19:3667–75.
29. Mittal K, Choi DH, Ogden A, Donthamsetty S, Melton BD, Gupta MV, et al. Amplified centrosomes and mitotic index display poor concordance between patient tumors and cultured cancer cells. Sci Rep 2017;7:43984.
30. Ward A, Hudson JW. p53-Dependent and cell specific epigenetic regulation of the polo-like kinases under oxidative stress. PLoS One 2014;9:e87918.
31. Farina AR, Tacconelli A, Cappabianca L, Cea G, Panella S, Chioda A, et al. The alternative TrkAIII splice variant targets the centrosome and promotes genetic instability. Mol Cell Biol 2009;29:4812–30.
32. Yu Z, Mouillesseaux KP, Kushner EJ, Bautch VL. Tumor-derived factors and reduced p53 promote endothelial cell centrosome over-duplication. PLoS One 2016;11:e0168334.
33. Cui SY, Huang JY, Chen YT, Song HZ, Huang GC, De W, et al. The role of Aurora A in hypoxia-inducible factor 1alpha-promoting malignant phenotypes of hepatocelluar carcinoma. Cell Cycle 2013;12:2849–66.
34. Fanale D, Bazan V, Corsini LR, Caruso S, Insalaco L, Castiglia M, et al. HIF-1 is involved in the negative regulation of AURKA expression in breast cancer cell lines under hypoxic conditions. Breast Cancer Res Treat 2013;140:505–17.
35. Mittal K, Choi DH, Wei G, Kaur J, Klimov S, Arora K, et al. Hypoxia-induced centrosome amplification underlies aggressive disease course in HPV-negative oropharyngeal squamous cell carcinomas. Cancers 2020;12:517.
36. Mittal K, Choi DH, Klimov S, Pawar S, Kaur R, Mitra AK, et al. A centrosome clustering protein, KIFC1, predicts aggressive disease course in serous ovarian adenocarcinomas. J Ovarian Res 2016;9:17.
37. Mittal K, Donthamsetty S, Kaur R, Yang C, Gupta MV, Reid MD, et al. Multinucleated polyploidy drives resistance to Docetaxel chemotherapy in prostate cancer. Br J Cancer 2017;116:1186–94.
38. Eustace A, Mani N, Span PN, Irlam JJ, Taylor J, Betts GNJ, et al. A 26-gene hypoxia signature predicts benefit from hypoxia-modifying therapy in laryngeal cancer but not bladder cancer. Clin Cancer Res 2013;19:4879–88.
39. Lopes CAM, Mesquita M, Cunha AI, Cardoso J, Carapeta S, Laranjeira C, et al. Centrosome amplification arises before neoplasia and increases upon p53 loss in tumorigenesis. J Cell Biol 2018;217:2353–63.
40. Godinho SA, Pellman D. Causes and consequences of centrosome abnormalities in cancer. Philos Trans R Soc Lond B Biol Sci 2014;369;20130467.
41. Maniswami RR, Prashanth S, Karanth AV, Koushik S, Govindaraj H, Mullangi R, et al. PLK4: a link between centriole biogenesis and cancer. Expert Opin Ther Targets 2018;22:59–73.
42. Bruno T, Valerio M, Casadei L, De Nicola F, Goeman F, Pallocca M, et al. Che-1 sustains hypoxic response of colorectal cancer cells by affecting Hif-1alpha stabilization. J Exp Clin Cancer Res 2017;36:32.
43. Zhang J, Wang C, Chen X, Takada M, Fan C, Zheng X, et al. EglN2 associates with the NRF1-PGC1alpha complex and controls mitochondrial function in breast cancer. EMBO J 2015;34:2953–70.
44. Agrawal AK, Seth PK, Squibb RE, Tilson HA, Uphouse LL, Bondy SC. Neurotransmitter receptors in brain regions of acrylamide- treated rats. I: Effects of a single exposure to acrylamide. Pharmacol Biochem Behav 1981;14:527–31.
45. Schödel J, Oikonomopoulos S, Ragoussis J, Pugh CW, Ratcliffe PJ, Mole DR. High-resolution genome-wide mapping of HIF-binding sites by ChIP-seq. Blood 2011;117:e207–17.
46. Wingender E, Dietze P, Karas H, Knuppel R. TRANSFAC: a database on transcription factors and their DNA binding sites. Nucleic Acids Res 1996;24:238–41.
47. Sabat-Pospiech D, Fabian-Kolpanowicz K, Prior IA, Coulson JM, Fielding AB. Targeting centrosome amplification, an Achilles' heel of cancer. Biochem Soc Trans 2019;47:1209–22.
48. Brahimi-Horn MC, Pouyssegur J. Harnessing the hypoxia-inducible factor in cancer and ischemic disease. Biochem Pharmacol 2007;73:450–7.
49. Ogden A, Rida PC, Aneja R. Prognostic value of CA20, a score based on centrosome amplification-associated genes, in breast tumors. Sci Rep 2017;7:262.
50. Fischer M, Quaas M, Steiner L, Engeland K. The p53-p21-DREAM-CDE/CHR pathway regulates G2/M cell cycle genes. Nucleic Acids Res 2016;44:164–74.
51. Lee MY, Moreno CS, Saavedra HI. E2F activators signal and maintain centrosome amplification in breast cancer cells. Mol Cell Biol 2014;34:2581–99.
52. Lohse I, Mason J, Cao PM, Pintilie M, Bray M, Hedley DW. Activity of the novel polo-like kinase 4 inhibitor CFI-400945 in pancreatic cancer patient-derived xenografts. Oncotarget 2017;8:3064–71.
53. Wong YL, Anzola JV, Davis RL, Yoon M, Motamedi A, Kroll A, et al. Cell biology. Reversible centriole depletion with an inhibitor of polo-like kinase 4. Science 2015;348:1155–60.
54. Denu RA, Shabbir M, Nihal M, Singh CK, Longley BJ, Burkard ME, et al. Centriole overduplication is the predominant mechanism leading to centrosome amplification in melanoma. Mol Cancer Res 2018;16:517–27.
55. Soni S, Padwad YS. HIF-1 in cancer therapy: two decade long story of a transcription factor. Acta Oncol 2017;56:503–15.
56. Shin DH, Chun YS, Lee DS, Huang LE, Park JW. Bortezomib inhibits tumor adaptation to hypoxia by stimulating the FIH-mediated repression of hypoxia-inducible factor-1. Blood 2008;111:3131–6.